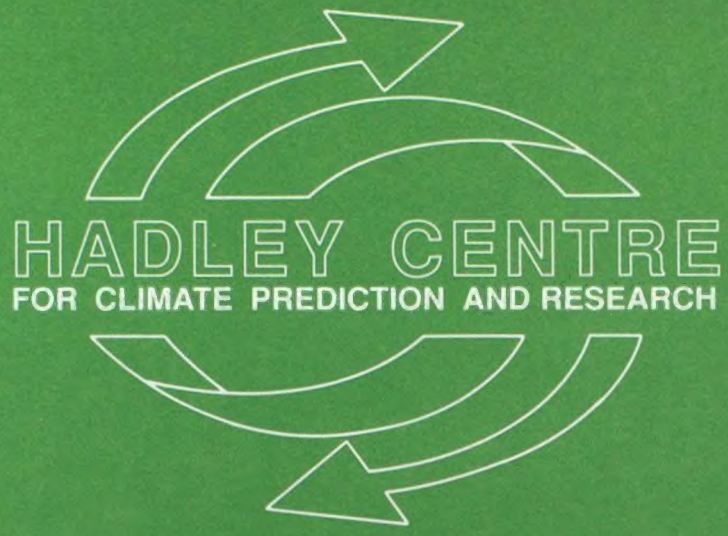

Worldwide ocean-atmosphere surface fields in Sahel wet and dry years using provisionally corrected surface wind data.

by

M. N. Ward

CRTN 20

November 1991

CLIMATE
RESEARCH
TECHNICAL
NOTE

Hadley Centre
Meteorological Office
London Road
Bracknell
Berkshire RG12 2SY

CLIMATE RESEARCH TECHNICAL NOTE NO. 20

WORLDWIDE OCEAN-ATMOSPHERE SURFACE FIELDS IN SAHEL WET AND DRY YEARS USING PROVISIONALLY CORRECTED SURFACE WIND DATA

by

M NEIL WARD

Hadley Centre for Climate Prediction and Research
Meteorological Office
London Road
Bracknell
Berkshire RG12 2SY
U. K.

NOTE: This paper has not been published. Permission to quote from it should be obtained from the Director of the Hadley Centre.

ABSTRACT

Worldwide ship datasets of sea surface temperature (SST), sea level pressure (SLP) and surface vector wind are analyzed for a July-September composite of five Sahel wet years (1950, 1952, 1953, 1954, 1958) minus five Sahel dry years (1972, 1973, 1982, 1983, 1984) (**W-D**). The results are compared with fields for 1988 minus 1987 (**88-87**); Sahel rainfall in 1988 was near the 1951-80 normal, whereas 1987 was very dry. Before performing the analyses, an extensive study of the geostrophic consistency of trends in pressure gradients and observed wind was undertaken, motivated by the suggestion that changes in observational practice on board ships have introduced an upward trend in reported wind speed over the last 40 years.

Over the period 1949-1988, the results suggest that there is a mean increase in reported wind speed of about 16% that *cannot* be explained by trends in geostrophic winds derived from seasonal mean SLP. Estimates of the wind bias are averaged for 18 ocean regions. The trend in every 2^{o} lat x 2^{o} long wind time series is adjusted according to the mean bias of the region in which the box resides.

The **W-D** Sahel composite shows coherent atmospheric variations in many oceanic regions, which is consistent with recent suggestions that worldwide SST variations force much of the variability in seasonal Sahel rainfall. The atmospheric fields suggest wetter years in the Sahel are often accompanied by a stronger Indian monsoon, enhanced annual cycle in the tropical Pacific, and low SLP in the tropical western Pacific near New Guinea. There is also a strong suggestion of increased cyclonicity in the extra-tropical North Atlantic / Northwest Europe sector. All the above features were also present in **88-87** fields.

In the tropical Atlantic, **W-D** shows many of the features identified by previous authors. However, the **88-87** fields *do not* reflect these large scale changes. Instead there is only local strengthening of the pressure gradient and wind flow from Brazil to Senegal. The **88-87** fields seem to provide an example of processes outside the tropical Atlantic acting as the primary cause of rainfall variations in the Sahel.

1. Introduction

The Sahel region of Africa (Fig. 1a) receives 80-90% of its annual rainfall in the months July-September. The large interannual and interdecadal variability in the seasonal rainfall (Fig. 1b) demands explanation, and various mechanisms have been proposed (reviewed by Druyan 1989). Variations at the ocean-atmosphere interface of the tropical Atlantic are clearly associated with the rainfall variability (Lamb 1978, Hastenrath 1984, Lough 1986) but Folland et al (1986, 1991), Palmer (1986) and Rowell et al (1991) have argued that Sea Surface Temperature (SST) in all the major ocean basins forces Sahel rainfall variations. This paper identifies some of the surface atmospheric variations over the global oceans that accompany the variations in SST and Sahel rainfall. A further purpose of the paper is to estimate the extent to which results are influenced by any evolving bias in ship wind speed reports (Ramage 1987, Cardone et al 1990). This is achieved by forming a new wind dataset in which wind trends in the period 1949-1988 are forced to be geostrophically consistent with trends in surface pressure gradients.

2. Data

a. Rainfall

The annual standardized Sahel rainfall anomaly series used in this study (Fig. 1b) is based on Nicholson (1985). For values since 1984, the series has been updated using available CLIMAT reports (details of the updating method are in Colman (1988)).

b. Surface Atmosphere

COADS 2° lat x 2° long (2x2) trimmed monthly means for the years 1949-1988 were used for the analyses (Woodruff et al 1987). Data were further processed as follows:-

(i) For a comparison of geostrophic and observed winds

Monthly means of sea level pressure (SLP), zonal wind component (u), meridional wind component (v), and wind speed for 1949-1988 were all used. The following details about the monthly means were also used: number of observations, standard deviation of the observations, mean day of the observations in the

month, mean location of the observations within the 2x2 box. Currently, data for 1980-1988 contain only the mean and number of observations for each of the meteorological parameters. To overcome this deficiency, a mean of each of the missing details (except day of the month) was calculated for 1960-79 and these were used for the 1980-88 data. To improve data coverage, the monthly dataset was transformed into a dataset of three-month seasons, using:-

$$V_s = \frac{\sum_{m=1}^{3} V_m N_m}{\sum_{m=1}^{3} N_m} \qquad (1)$$

where V_s is the value for season s, V_m is the value of variable V in month m, N_m is the number of observations in month m, and summation is over the three months that constitute the season.

(ii) For studying relationships with Sahel rainfall

The monthly COADS data for SLP, u and v were combined into a July-September dataset applying the same principle as Eq. (1). Mean values (normals) were calculated for the period 1969-1988, the period with best data coverage. To calculate the normals, the data were initially averaged over 2° lat x 4° long (2x4) boxes, to improve data coverage. At least 8 observations were required for a 2x4 box to have a seasonal value in a given year. To calculate a normal, at least 15 out of the 20 seasons 1969-1988 were required to have a seasonal value. The boxes were overlapped by 2° longitude. Longitudinally adjacent 2x4 normals were averaged, giving a set of 2x2 normals with effectively a 1:2:1 smoothing in the longitudinal direction.

Anomaly datasets on the 2x2 scale were created for the July-September seasons 1949-1988. Results in this study are presented on the 10° lat x 10° long (10x10) scale. The 10x10 seasonal anomaly dataset was formed:-

$$V_{10*10} = \frac{\sum_{i=1}^{25} V_i N_i}{\sum_{i=1}^{25} N_i} \qquad (2)$$

where V_{10*10} is the 10x10 anomaly for variable V, V_i is the seasonal anomaly of V, and N_i is the number of observations in the i^{th} constituent 2x2 box. A maximum value of 100 was set for N_i, so that the (rare) 2x2 boxes that have many more than 100 observations in a season do not dominate the estimate of the

10x10 seasonal anomaly. For inclusion in the 10x10 dataset, at least 20 observations were required for the 10x10 box as a whole. The optimum way of combining the 2x2 anomalies to achieve the *best estimate* 10x10 anomaly will be a weaker function of N_i than in Eq. (2). The weighting in Eq. (2) effectively assumes that the seasonal anomaly being estimated is uniform across the 10x10 box, i.e. the effective number of independent 2x2 boxes is 1. A common alternative to Eq. (2) is to give each 2x2 anomaly equal weight. However, the approximation in Eq. (2) is particularly useful in regions where data coverage is dominated by narrow shipping lanes (e.g. tropical South Atlantic) where the number of observations in adjacent 2x2 boxes for a season may vary from over 100 to less than 5. In such a situation, considerably more weight should be given to the 2x2 anomaly based on over 100 observations.

c. Sea Surface Temperature

SST data were taken from the Meteorological Office Historical Sea Surface Temperature data set version 4 (MOHSST4) (Bottomley et al 1990) which contains monthly SST anomalies, where available, for 5° lat x 5° long (5x5) grid boxes extending over the world's oceans. The 5x5 monthly values for July, August and September were averaged with equal weight into a 10x10 seasonal dataset for July-September. As little as one constituent monthly 5x5 monthly anomaly was allowed when calculating a seasonal 10x10 anomaly.

3. Corrections for the wind dataset

a. Background

Cardone et al (1990) suggest that the wind speed reported by ships has increased in recent decades due to changes in observational practices. The main cause that they identify is an increasing fraction of anemometer readings, typically now made at a mean height of 20m, relative to Beaufort force estimates, which are converted to 10m winds before insertion into computerized datasets like COADS. So before studying the relationship between Sahel rainfall and surface winds, an attempt has been made to verify the presence of Cardone et al's wind trend in all ocean areas, and where necessary to remove the spurious trend from the data. To achieve this, trends in seasonal mean vector winds are compared with trends in seasonal mean pressure gradients, and the results are tested for consistency based on the geostrophic wind relation. A preliminary study by Wright (1988) on an area in the tropical Pacific suggested that trends in

reported wind speeds in that area were unlikely to be real because they were not supported by changes in surface pressure gradients. A wind correction method based on this approach assumes that there is no substantial time-varying bias in the estimated pressure gradients (Appendix A), and that the difference between geostrophic wind trend and observed wind trend can be used to isolate time-varying bias in wind observation. The derived geostrophic wind is a function of pressure difference, so will largely be independent of any time-varying bias that may exist in ship pressure data, though other problems such as changes in bias towards reports during fair weather may influence the geostrophic wind trends in some regions. The geostrophic wind is not a good approximation to the true wind near the equator. It was found that within 4° latitude of the equator, the correlation between geostrophic and observed wind over the 40 years analyzed was close to zero, so these series were excluded from the analysis. All series polewards of 4° were included, but the contribution of each 2x2 box to the overall results was weighted according to the correlation between the geostrophic and observed wind, thereby ensuring that little weight was given to those boxes where the derived geostrophic wind seemed to provide a poor approximation of the true wind.

b. Quantifying the discrepancy between wind and pressure gradient trends

Where possible, an estimate of the seasonal mean geostrophic wind in a given direction α' ($G_{\alpha'}$) is made from the COADS seasonal mean SLP (see Appendix A for details). Each estimate of $G_{\alpha'}$ is adjusted for friction and other ageostrophic wind components to yield $\tilde{G}_{\alpha'}$. $\tilde{G}_{\alpha'}$ is compared with the corresponding V_{α}, the observed seasonal vector wind in direction α, where α differs from α' by 15° to allow for backing of the wind due to friction. (15° is a generally accepted value (e.g. Riehl 1979), but its choice here is not critical, and results reported were largely unchanged by setting the backing angle to 0°). Below, trends in V_{α} and $\tilde{G}_{\alpha'}$ are compared only in those 2x2 boxes that had a mean seasonal vector wind (over 1949-1988) $\overline{V_{\alpha}} < -1$ m s^{-1} or $> +1$ m s^{-1}, so that the vector trends can provide approximations for the percentage increase in the magnitude of the wind speed (see Appendix B).

For most 2x2 boxes, the direction α was close to the longitudinal direction. This choice of analyzing zonal wind reflects the preference for the 2x2 boxes to have $\overline{V_{\alpha}}$ as different from zero as possible (Appendix B). However, in narrow shipping lanes, α was chosen so that the required pressure gradient to estimate $\tilde{G}_{\alpha'}$ was directed approximately along the shipping lane, hence permitting maximum use of the available

SLP data (see Appendix A).

For every 2x2 ocean box included in the analysis, and (separately) for each of the four seasons, the following linear model was fitted:

$$(V_\alpha - \tilde{G}_{\alpha'})_t = a_0 + a_1 t + \epsilon \qquad (3)$$

where $(V_\alpha - \tilde{G}_{\alpha'})_t$ is the difference between the observed and geostrophic seasonal wind in year t, ϵ is white noise with mean 0, a_0 is a constant and a_1 represents the trend in the difference between V_α and $\tilde{G}_{\alpha'}$. Usually a_1 is fitted using a least squares procedure. However, the magnitude of the fitted parameter is then biased low by observational error on the variables (Kendal and Stuart, 1961, p413). To avoid this, a_1 was estimated:

$$a_1 = \frac{\overline{(V_\alpha - \tilde{G}_{\alpha'})}_2 - \overline{(V_\alpha - \tilde{G}_{\alpha'})}_1}{\bar{t}_2 - \bar{t}_1} \qquad (4)$$

where overbar indicates quantities meaned over period 1 = 1949-1968, 2 = 1969-1988. Only those years with an estimate of V_α and $\tilde{G}_{\alpha'}$ were included, and only 2x2 boxes with estimates in at least 50% of years in period 1 and period 2 were included. In terms of the process in Eq. (3), $\overline{(V_\alpha - \tilde{G}_{\alpha'})}_i$ is an unbiased estimate of $(V_\alpha - \tilde{G}_{\alpha'})$ at $t=\bar{t}_i$. The slope of the line joining the two unbiased estimates of the process at $\bar{t}_1$ and $\bar{t}_2$ (Eq. (4)) gives an unbiased estimate of the trend a_1 (units are m s^{-1} yr^{-1}). The implied spurious percentage increase S in the observed wind vector over 40 years is

$$S = \left(\frac{a_1 * 40}{\bar{V}_\alpha}\right) * 100 \qquad (5)$$

Two criteria were identified which influence the degree of confidence attributed to each a_1:

(i) Number of years with data: N = number of years with an estimate of $(V_\alpha - \tilde{G}_{\alpha'})$

(ii) Meteorological reliability: A simple estimate of this is given by the correlation r between V_α and $\tilde{G}_{\alpha'}$. The correlation may be low due to noise in the data or due to geostrophy providing a poor approximation to the real wind. In either case, confidence in S is reduced. Note that the magnitude of spurious trend proposed by Cardone et al is sufficiently small to have little impact on r.

Combining the above two considerations, each spurious trend S was allotted a weight equal to $N*r$. The

weighted average of S over all seasons and 2x2 boxes is 16.1%, which is the correct order of magnitude to support Cardone et al; 16.1% is the increase predicted by Cardone et al for a change in the percentage of anemometer readings from 0% in 1949 to 60% in 1988, in a neutral boundary layer and mean wind speed of 5 m s^{-1}.

As a first attempt to derive geographically varying estimates of S, the values have been averaged over the regions shown in Fig. 2. It was assumed that changes in observational practice, and therefore the required corrections to the data, would be more coherent within shipping lanes than between shipping lanes. So the divisions in Fig. 2 attempt to include shipping lanes in the same region. Regional divisions were also made where marked and coherent variations in the values of S were noted (e.g. extratropical North Atlantic). Finer resolution or more objective selection of the regions was not thought justified at this stage. Equatorwards of 4° latitude, no estimates of S were made, but equatorial regions are allotted to a region in Fig. 2 for the purpose of correcting the whole wind dataset in the next section. Most equatorial 2x2 boxes were allotted to the nearest region. The few exceptions (e.g. in the eastern tropical Pacific) were made so as to avoid the allocation of a 2x2 box to a region that was clearly dominated by a different shipping lane.

Of the 18 regions in Fig. 2, 13 have mean values of S in the range +10% to +25%. North of 50°N, the spurious wind trend actually appears negative, especially in the Atlantic. This negative trend is present in the different geostrophic analyses performed (not shown) with different length scales for estimating the pressure gradients, different data inclusion criteria etc. Those areas which Cardone et al studied (marked with crosses on Fig. 2) all show positive values for S.

c. Correcting the wind data

Figure 2 indicates that trends in the estimated pressure gradients and trends in the observed winds are not geostrophically consistent. Cardone et al have presented a strong argument for time-varying bias in reported wind speeds, a bias that is of the right order of magnitude to explain most of the results in Fig. 2. Other possible explanations, such as a genuine change in the ratio of geostrophic to ageostrophic wind, or a time-varying bias in the pressure gradient estimates, are unlikely to be able to explain the size of the values of S in Fig. 2. Thus, to a first approximation, the values of S are interpreted as isolating a spurious

trend in the wind data. For studying relationships with Sahel rainfall in the next section, a corrected July-September wind dataset has been calculated using the results in Fig. 2. For each 2x2 vector wind time series, the corrected data are calculated:

$$\tilde{u}_t = u_t - [u_t * (S/100) * (t - t_b)/40]$$
$$\tilde{v}_t = v_t - [v_t * (S/100) * (t - t_b)/40] \qquad (6)$$

where $\tilde{u}_t$ and $\tilde{v}_t$ are the corrected u and v seasonal wind vectors for time t, u_t and v_t are the observed COADS seasonal wind vectors for time t, and S is the 1949-88 mean spurious percentage change in wind speed for the region (Fig. 2) in which the 2x2 box resides. Note that the mid-point of the season is used for t (e.g. July-September 1949, t=1949.71). t_b is an arbitrarily selected time which acts as the base time for the corrections. For example, if t_b=1949.0, then when t=1949.0, $\tilde{u}=u$ and $\tilde{v}=v$; 40 years later when t=1989.0, the wind vectors are reduced in magnitude by S%, (or increased by S% if S is negative). To correct the dataset for use in the next section on Sahel rainfall, t_b was set to the mid-point of the 1969-1988 July-September normals period (1979.2). To illustrate the impact of the corrections on the 10x10 anomaly dataset, Fig. 3 compares July-September anomalies of u and $\tilde{u}$ for a box in the trade wind regime of the tropical North Atlantic. There is a strong negative trend in u, corresponding to a strengthening of the reported easterly wind component, whereas the corrected wind time series $\tilde{u}$ has no significant trend. A time series of the difference in SLP anomaly in the boxes to the north and south (crosses in Fig. 3) contains no significant trend, so no trend in the July-September zonal wind is consistent with geostrophy. This result is highly dependent on there having been no trend in the mean location of the pressure observations in the 10x10 boxes; the geostrophic analyses described earlier in this section were more rigorous because they used data averaged over smaller boxes and, when possible, allowed for the mean location of the observations (see Appendix A).

4. Sahel wet and dry years

Folland et al (1986) calculated the difference in SST for the five wettest and five driest Sahel years (W-D) in the period 1950-1984. Figure 4 compares the SST composite map (here recalculated using the new version of MOHSST, see section 2) with corresponding maps for SLP and surface vector wind. At least eight out of the ten years were required to have data for a 10x10 box to be included. The local statistical significance of the SST and SLP differences is assessed using a t-test (Afifi and Azen 1979). Maps for 1988

minus 1987 are also presented (88-87, Fig. 5); 1988 and 1987 represent two recent years with a considerable difference in Sahel rainfall (1988 much wetter than 1987, Fig. 1b). To confirm that the SLP composite map is providing a representative summary of the relationship between SLP and Sahel rainfall, a correlation map is presented (Fig. 6) showing the correlation between SLP and Sahel rainfall over the whole period 1949-1988. The statistical significance of each correlation is assessed using a t-test, allowing for serial correlation when estimating the degrees of freedom (Bartlett 1935).

Tropical North Atlantic

In W-D, close to Africa at 10°-30°N, negative SLP values are bordered by relatively higher values equatorwards and near 35°N. The corresponding wind pattern is consistent, with enhanced convergence near and to the north of the latitude of the Sahel, resulting mainly from southerly flow, but with some enhanced northeasterly around 35°N as well. In 88-87, widespread low SLP is not found. However, confined to the eastern side of the basin, the meridional pressure gradients are directed into a belt near 20°N, and the wind flow is consistent with this showing enhanced convergence around 20°N resulting from enhanced southerly flow from the south and enhanced northeasterly flow from the north.

In 88-87, negative SST values prevail throughout the tropical North Atlantic, *opposite* to that found for W-D (Fig. 4a and Folland et al 1986), and in other studies (e.g. Lamb 1978). Furthermore, there is *no* similarity between the SLP and wind fields in Figs. 4 and 5 away from the extreme eastern side of the basin.

The wind corrections have a large impact at 15°N on the western side of the basin in W-D. The raw data suggest a substantial weakening of the trade winds in wet years, but the corrections leave only a slight weakening.

Tropical South Atlantic

In both W-D and 88-87, the region close to Brazil has low SST, and high SLP. In W-D the raw wind data suggest a small enhancement of the cross equatorial flow near Brazil, whereas the corrected data show a stronger southerly flow that is similar to that which occurred in 88-87. The similarity in the cross equatorial pressure gradient near Brazil in W-D and 88-87 makes the corrected wind the more plausible.

In 88-87, positive SST values prevail in the rest of the tropical South Atlantic, *opposite* to that found in W-D (Fig. 4a and Folland et al 1986). In terms of the cross-equator dipole of tropical Atlantic SST anomalies that Lough (1986) related to Sahel rainfall, 1988 should have been drier than 1987 in the Sahel, not wetter (Fig. 1b).

In W-D, the high SLP near Brazil extends to a statistically significant high centre near 35°S, 10°W. This produces a northward pressure gradient over much of the tropical South Atlantic west of 0°. In the corrected wind data, the flow suggests a large scale strengthening of the Southern Hemisphere trade winds over these longitudes. In 88-87, both the SLP and wind suggest that *no* such large scale enhancement occurred. So in the tropical South Atlantic, the SST and the surface atmospheric features in W-D are very different from those in 88-87, except for close to Brazil. Indeed, the region close to Brazil is the only part of the tropical South Atlantic that has statistically significant linear correlations between SLP and Sahel rainfall over the years 1949-1988 (Fig. 6).

Extratropical North Atlantic

In W-D, positive SST values exist throughout the extratropical North Atlantic, except close to the UK and the Iberian peninsula. The positive values are statistically significant near Greenland and at about 35°N. However, the cooling in the North Atlantic near Greenland, observed over the last two decades (Folland et al 1990), showed no sign of reversal in 1988; indeed 1988 was actually colder than 1987 in this region.

In W-D, the main feature of the atmospheric maps is a statistically significant negative SLP region near the UK, with accompanying cyclonic circulation. This association is also statistically significant when measured using correlation coefficients for 1949-1988 (Fig. 6). Furthermore, in 88-87, strong cyclonic circulation is present near the U.K., though in addition there are also large positive SLP values in the western sub-tropics, where large positive SST values are also found.

Mediterranean / Red Sea

In W-D, the whole Mediterranean has high SST and low SLP. There are similar values in 88-87 in the eastern Mediterranean, where statistical significance is found in Figs. 4 and 6. The transition from positive to negative SST values in the Red Sea occurs in almost the identical position in W-D and 88-87.

Indian Ocean

In W-D *and* 88-87, SLP values decrease by about 1.0-1.5mb from the equatorial African coast to the coast of the Indian sub-continent. Enhanced Indian monsoon flow is expected from such a pressure gradient. Enhanced monsoon flow is found in the 88-87 map and in the corrected data for W-D, but not in the raw data for W-D. This gives further support to the corrected wind data.

The statistically significant low SLP north of the equator in W-D is accompanied by statistically significant positive SLP south of the equator, just north of the climatological centre of the Mascarene high. The pressure gradient across the equator appears enhanced. An enhanced cross equatorial flow is therefore expected, but this is not present, even in the corrected data. However, the equator marks a boundary in the regions used for the wind corrections; if the corrections had been smoothed across this boundary, the data just to the south of the equator would have had substantially larger corrections applied (Fig. 2), making them more consistent with the SLP in W-D.

Except in parts of the western Indian Ocean and close to the African coast, the negative SST values of W-D are also found in 88-87. However, the stronger Mascarene high and easterly winds of W-D are the direct opposite of the low SLP and stronger westerlies in 88-87. Over the whole 40 year period, there is no statistical correlation between July-September SST and surface atmospheric features in this region. This suggests either that there is little ocean-atmosphere interaction on a seasonal time scale in this region, or that the data are too unreliable to detect the interaction, or that the interaction is more complex. This could occur if the Mascarene High was remotely as well as locally forced. Over 1949-1988, the average association between the Mascarene High and Sahel rainfall is actually quite weak (Fig. 6) despite its statistical significance in W-D. It is the negative correlations between Sahel rainfall and SLP in the North Indian Ocean that are highly significant.

Pacific Ocean

Fields for 88-87 are dominated by the switch from El Nino (1987) to La Nina (1988) that occurred in boreal spring 1988. It is known that the overall statistical link between ENSO and rainfall in the Sahel is fairly weak (Ropelewski and Halpert 1987, 1989). However, this might not be true for certain types of ENSO variations. The period 1987 to 1988 was remarkable for the very great and rapid transition between strong El Nino (1987) and strong La Nina (1988). It is therefore important to consider more closely

features of the 88-87 maps in the Pacific that may have caused this particular ENSO cycle to have a pronounced impact on the difference in Sahel rainfall between the two years. This possibility is enhanced by the apparently inconsistent changes in SST in the Atlantic between W-D and 88-87 discussed previously.

The 88-87 SST field has a very strong gradient directed north to south near 5°N over the longitudes 110°-170°W. This is accompanied by a strong south to north SLP gradient and southerly wind flow. These features, albeit much weakened, are present in the W-D SST SLP and (corrected) wind fields. In the western equatorial Pacific the 88-87 SST field has another strong gradient, this time principally directed west to east, resulting from large negative SST values in the central equatorial Pacific and large positive values near New Guinea, which form a local maximum in the SST difference values. The W-D SST field does also have a relative maximum of SST values near New Guinea, but the magnitudes are much weaker than in 88-87. However, the atmospheric features in W-D and 88-87 are remarkably similar over these longitudes. Both have a pair of low pressure areas centred near New Guinea and in the China Sea near 30°N. Convergence into the China Sea low pressure trough is further enhanced in both fields by high SLP values to the east. Though this arrangement of SLP in the western Pacific is only marginally statistically significant in W-D, correlations between SLP and Sahel rainfall over 1949-1988 identify the pattern as highly statistically significant (Fig. 6). This pattern of atmospheric variation is related to, but is not synonymous with, the Southern Oscillation. Links between ocean-atmosphere variations in the Pacific and Sahel rainfall may therefore be stronger than the relatively weak empirical associations measured between ENSO and Sahel rainfall. General circulation model (GCM) experiments have also suggested that the empirical relationship with ENSO underestimates the importance of the Pacific for Sahel rainfall (Folland et al 1991).

5. Discussion and Conclusions

Surface atmospheric variations over the oceans have been identified for the composite of Sahel wet years (1950, 1952, 1953, 1954, 1958) minus dry years (1972, 1973, 1982, 1983, 1984) (W-D) that were previously studied by Folland et al (1986) in the context of worldwide SST variations. In addition, fields for 1988 minus 1987 (88-87) have been presented, to identify candidates for causing the dramatic return in 1988 of rainfall totals nearer to the 1951-80 normal. The W-D composite contains clues to processes that operate on interdecadal and interannual timescales. Other authors have started to separate the processes

empirically using various types of empirical orthogonal function (EOF) analysis (Lough 1986, Wolter 1989, Folland et al 1991). All these studies identified a mode in the tropical Atlantic that was mainly related to short period (< 5 years) variability in Sahel seasonal rainfall. Wolter also included the tropical Indian Ocean in his analyses, and found SST here to be involved in a mode that operated mainly on interdecadal timescales. This mode is probably part of an inter-hemispheric variation of SST, an idea introduced in Folland et al (1986) and isolated as the third EOF of worldwide SST variations in Folland et al (1991). Wolter's EOF included atmospheric data as well, but may have been influenced by the problem in wind speed data discussed in section 3. In particular, implicit in Wolter's long-time scale EOF is the suggestion that a stronger Indian monsoon tends to accompany reduced rainfall in the Sahel, whereas the opposite is suggested in 88-87 and the corrected version of W-D.

Table 1 Differences in Sahel rainfall and SST EOFs for selected sets of years.

	Sahel Rainfall	SST EOF2	SST EOF3	SST REOF2
W-D	+3.14*	-0.74	-2.04*	-2.53*
88-87	+1.71	-3.10	-1.15	+0.92

Notes:
Values in the Table are of annual Sahel rainfall (Fig. 1b) and the July-September time coefficients of the SST EOFs (Fig. 7); units are standard deviations (all four series were standardised to have mean of zero and standard deviation of 1 for 1949-1988)
W-D = average values for (1950, 1952, 1953, 1954, 1958) minus (1972, 1973, 1982, 1983, 1984). * = difference is statistically significant at 1% level.
88-87 = values for 1988 minus 1987.

The three SST EOFs that Folland et al (1991) discuss in relation to Sahel rainfall are shown here in Fig. 7. The July-September time coefficients of these EOFs have been standardised over the period 1949-1988, and the mean difference in the values has been calculated for W-D and 88-87 (Table 1). The W-D composite (Fig. 4a) contains a strong component of inter-hemispheric variation in SST (Northern Hemisphere warmer than Southern Hemisphere). The very negative W-D coefficient difference for EOF3 (Table 1) reflects this. The EOF3 difference for 88-87 is also negative (Table 1), but this is unlikely to explain all the rainfall difference (also shown in Table 1), especially since Folland et al (1991) show that EOF3 is mainly related to low frequency variations in Sahel rainfall, not large interannual fluctuations, such as occurred in 88-87.

The 88-87 fields in Fig. 5 *do not* show the large scale tropical Atlantic features found in W-D and in other studies of Sahel rainfall variability. The SST rotated EOF2 (Fig. 7b) that Folland et al (1991) use to represent the relationship between Sahel rainfall and tropical Atlantic SST, has for 88-87 a slightly positive value, in contrast to the statistically significant negative value for W-D (Table 1). It seems the causes of the return to nearer normal rainfall in 1988 lie outside the tropical Atlantic. The SST EOF (Fig. 7c) that Folland et al (1991) use to represent El Nino does show a very large difference 88-87, consistent with the ENSO variation that occurred in these years. However, as previously noted, there is only a weak link between measures of ENSO (such as this EOF) and Sahel rainfall; the difference in the coefficient for W-D is not statistically significant (Table 1).

The particular type of atmospheric surface pattern in 88-87 in the tropical Indian and Pacific Oceans *does* resemble closely the pattern of variability that Meehl (1987) identified in relation to stronger Indian monsoons this century. The pattern in 88-87 of enhanced boreal summer annual cycle in the Indian and Pacific fields, plus low pressure near to and south of the equator in the tropical western Pacific, is in many respects repeated in W-D and in the SLP correlation map (Fig. 6), so there is a strong suggestion that the 88-87 pattern of seasonal variation through the tropics has occurred in the past with a similar association to Sahel rainfall. GCM integrations forced with the observed SST for 1987 and 1988 have successfully simulated substantially more rainfall in the Sahel in 1988 than in 1987 (Rowell et al 1991, Palmer et al 1991). So despite the weak empirical link, it seems that Pacific SSTs, acting in conjunction with SST in other ocean basins, must in some years have a major impact on Sahel rainfall, probably contributing to the establishment of the distinctive atmospheric anomaly pattern in the tropical western Pacific and a modified annual cycle throughout much of the tropics.

Analyses in this paper have used a surface wind dataset that has been provisionally corrected for time-varying bias in wind speed reports from ships. The estimates of bias (Fig. 2) support Cardone et al (1990) who argue for a careful appraisal of the methods of wind observation on ships. The bias estimates are based on comparisons of derived (mainly geostrophic) winds with reported winds. A more accurate derived wind incorporating ageostrophic components more rigorously, would justify calculation of corrections with better temporal and spatial resolution, improving upon the current corrections which are linear in time and uniform over large areas and all seasons of the year. Nonetheless, the current corrections provide useful quantification of the uncertainty in the ship wind data and of the impact the data problems may

have for detecting decadal climate variability. The impact of the corrections on the physical interpretation of the W-D Sahel composite is largest in the tropical Atlantic and Indian Oceans.

Recent research has presented a strong case, using empirical evidence and GCM experiments, for worldwide SST fields forcing much of the observed variation in seasonal Sahel rainfall. This paper has made a start at describing the worldwide atmospheric variations that accompany the worldwide SST variations. For the remote SST to be important, as suggested by Folland et al (1991), some of the remote worldwide atmospheric variations identified in W-D and 88-87 must have consequences for the dynamics of the Sahelian atmosphere. A combination of GCM and empirical study is needed to identify the nature of the teleconnecting mechanisms. That different large-scale mechanisms are important in different years is supported by the fact that distinctive seasonal rainfall anomaly types have been identified over sub-Saharan Africa (Nicholson 1980, Janicot in press), and by the ability of all the major ocean basins to force Sahel rainfall variations in GCMs (Palmer 1986, Folland et al 1991). Furthermore, regional-scale variations in rainfall anomalies within the Sahel itself appear related to ocean-atmosphere variability (Janicot in press, Ward et al 1990, and modelled by Druyan and Koster 1989). So further studies will need to consider which processes operate on the Sahel as a whole and which processes are regionally specific.

APPENDIX A

Calculating the seasonal mean geostrophic wind

To calculate geostrophic winds, estimates of pressure gradients are needed. These could be made by fitting a smoothed surface to the SLP data, but the resulting gradients may be systematically influenced by data reliability, so that through time, as data become more reliable, a trend in the estimated gradients may be introduced. This needs to be avoided if the geostrophic wind trend is to be treated as 'truth' in comparisons with observed wind trends. The basic strategy adopted involves applying the following process 120 times (once for every season 1949-1988) to every 2x2 ocean box:

(i) Search for the pair of 2x2 seasonal SLP values that provide the most reliable estimate of seasonal mean SLP gradient across the 2x2 box.

(ii) Calculate the geostrophic wind that the SLP gradient implies.

(iii) Make approximate adjustments to the geostrophic wind for friction and other ageostrophic

components.

In more detail, consider a pair of 2x2 boxes (see Fig. A1) yielding a seasonal pressure difference δP:

$$\delta P = P_a - P_b \qquad \text{(A1)}$$

where P_a is a seasonal mean SLP for a 2x2 box in COADS, and is taken as an estimate of the seasonal mean SLP at the mean location a of the observations through the season. P_b is the mean SLP for the same season in a nearby 2x2 box. An estimate of the pressure gradient at the mid-point (m) of the line joining a and b and in the direction (n) defined by the direction of the line joining a and b is

$$\nabla_n P = \frac{\delta P}{D} \qquad \text{(A2)}$$

where D is the distance between points a and b. For a particular 2x2 box i, surrounding pairs of boxes were analyzed in turn as candidates for providing a reliable estimate of the pressure gradient across box i. For a pair of boxes to qualify as candidates, the following criteria needed to be satisfied (see Fig. A1):

(i) P_a and P_b must both be based on at least five observations

(ii) The angle θ between the line joining a and b and the "preferred axis" must be less than 20°. With the exception of the regions identified in Fig. A2, the "preferred axis" is always 15° clockwise from north-south in the Northern Hemisphere (as in Fig. A1), and 15° anticlockwise in the Southern Hemisphere, so the pressure gradient along the preferred axis yields a geostrophic wind which can be compared with the observed zonal wind, assuming 15° backing of the geostrophic wind due to friction. The regions identified in Fig. A2 have data coverage mainly confined to narrow shipping lanes. To make best use of the SLP data in these regions, the preferred axis is orientated along the shipping lane.

(iii) the distance between a and b should be between 500-1000 km (effectively defining a length scale for the pressure gradient estimates)

(iv) the mid-point m of the line joining a and b should be within 200 km of the centre c of box i.

(v) the mean date of the observations that yielded P_a and P_b must not differ by more than 15 days.

To identify which of the qualifying pairs would provide the most reliable estimate of $\nabla_n P$, the standard error of $\nabla_n P$ was estimated as

$$SE(\nabla_n P)=\frac{[SE(P_a)^2+SE(P_b)^2]^{1/2}}{D} \quad \text{(A3)}$$

The SE on the estimate of mean SLP for point a is a function of the number and distribution of observations through the season, temporal SLP variability through the season, and spatial variability in the instantaneous SLP fields. The latter is the error introduced by assuming that all observations were taken at point a. Generally, the spatial variability over about 2° of latitude and longitude will be much less than temporal variability through the season, so spatial variability is ignored. In the absence of serial correlation and assuming P_a is an estimate of the mean of an infinite population, SE(P_a) is $\sigma(n)^{-0.5}$, where σ is the standard deviation of the observations and n is the number of observations. However, the SLP observations do contain serial correlation, and P_a is an estimate of a mean over a restricted time period (the season). Assuming missing data are randomly distributed through the sample, we can write following Parker (1984) and Kidson and Trenberth (1988):

$$SE=\left(\frac{\sigma}{\sqrt{n'}}\right)\left(1-\frac{n'}{N'}\right) \quad \text{(A4)}$$

n' (the effective sample size) is a function of the number of SLP observations (n), the finite population size (N) and the serial correlation in the SLP observations (r_i, the serial correlation at lag i):

$$n'=\frac{n}{1+\left(\frac{2n}{N^2}\right)([N-1]r_1+[N-2]r_2+\ldots\ldots)} \quad \text{(A5)}$$

N' (the effective finite population size) is given by

$$N'=\frac{N}{1+\left(\frac{2}{N}\right)([N-1]r_1+[N-2]r_2+\ldots\ldots)} \quad \text{(A6)}$$

These equations cannot be applied immediately because they assume that the population is a time series sampled at regular time intervals. The ship observations are sampled at irregular time intervals, and they are continuously distributed in space. However, a number of assumptions can be made to allow an approximation to the parameters needed for the above equations. Firstly, though the serial correlation will be a function of sampling interval, a first order autoregressive process with r_1=0.8 has been assumed throughout (consistent with Kidson and Trenberth, 1988). This is a reasonable estimate for SLP in most

ocean regions for a sampling interval of 12 hours. If the number of observations was less than 30, it was assumed that the finite population size was 60; N was linearly increased to 150 as n increased to 100. Any box with more than 100 observations was assumed to have had just 100. This practical choice was made to avoid the few boxes with many more than 100 observations dominating the results by always being selected to estimate the pressure gradients. More sophisticated statistical treatment viewing the time series as a sample of a continuous process would be more accurate, but the above procedure was judged adequate for identifying the most reliable pressure gradient estimate. Errors associated with the individual observations themselves (e.g. instrumental, human) are ignored since we can only assume that these will on average have the same statistical properties (mean, variance) for all nearby 2x2 boxes.

The pair of boxes yielding the smallest value for SE($\nabla_n P$) was used to estimate the geostrophic wind:

$$G_{e'} = \frac{-\nabla_n P}{f\rho} \qquad \text{(A7)}$$

where f is the coriolis force and ρ is the density of air (standard sea level value of 1.225 kg m^{-3} is assumed).

The true wind differs from the geostrophic wind due to various ageostrophic components. An adjustment to $G_{e'}$ has been made to allow for these in two stages:

(i) Friction reduces the true near-surface wind speed below the geostrophic wind speed; the magnitude of the 10m geostrophic wind including the effects of friction ($G_{e'_F}$) can be approximated as (Garratt 1977):-

$$G_{e'_F} = rG_{e'}$$
$$r = 1.91 f^{0.074} w^{-0.139} \qquad \text{(A8)}$$

where r is the ratio of the observed to geostrophic wind, and w is taken here to be the mean reported wind speed for box i in the season. The ratio of the geostrophic to observed wind is difficult to generalise for wind speeds less than about 4 m s^{-1}, when Eq. (A8) is inappropriate. For simplicity, when the mean wind speed is less than 4 m s^{-1}, the ratio r is assumed to be that calculated for a wind speed of 4 m s^{-1}.

(ii) Other ageostrophic components: Allowance was made for systematic departures of the $G_{e'_F}$ from the comparable observed vector wind by simply multiplying $G_{e'_F}$ by a constant to force the mean of the derived wind to be the same as the mean of the observed wind over the whole period 1949-1988:

$$\tilde{G}_{\alpha' i}=G_{\alpha' F}\left[\frac{\overline{V_\alpha}}{\overline{G_{\alpha' F}}}\right] \qquad \text{(A9)}$$

where $\overline{G_{\alpha' F}}$ is the mean of all the estimates of $G_{\alpha' F}$ that are made for box i in the 40 seasons 1949-1988, and $\overline{V_\alpha}$ is the mean of all the comparable observed winds in the 40 seasons, α differing from α' by 15° to make an approximate allowance for the impact of friction on the direction of the observed wind.

APPENDIX B

The relationship between trends in seasonal mean vector wind and seasonal mean scalar wind speed

Cardone et al (1990) argue that the scalar wind speed (i.e. magnitude of the wind speed) reported by ships has increased due to changes in observational practice. It is important to identify if and how vector trends (e.g. trend in the seasonal mean zonal wind) can be used as a good approximation for trends in wind speeds, since it is vector wind trends that must be verified against trends in the derived vector wind $\tilde{G}_{\alpha' i}$ in Appendix A.

Consider sampling an identical season twice with an identically timed set of reports using (a) Beaufort estimates (b) anemometer readings. Following Cardone et al, the difference between each pair of identically timed reports will be a moderately non-linear function of stability and wind speed. However, for simplicity, assume that each anemometer wind speed report w_a is always larger than the Beaufort wind speed report w_b by the same percentage amount S:

$$w_a=w_b+\frac{S}{100}w_b \qquad \text{(B1)}$$

The corresponding zonal wind reports will be:

$$\begin{aligned} u_a&=w_a\sin\theta \\ u_b&=w_b\sin\theta \end{aligned} \qquad \text{(B2)}$$

where θ is the angle of the wind measured clockwise from north. Substituting between Eqs. (B1) and (B2), it follows that:

$$u_a = u_b + \frac{S}{100} u_b \qquad \text{(B3)}$$

Equation (B3) shows that the modulus of the anemometer vector wind has the same percentage increment as the anemometer wind speed. So over a period of time, an increase in the ratio of anemometer to Beaufort reports will yield the same percentage increase S in the seasonal wind speed (w) and the modulus of the seasonal vector wind ($|V|$). In principle, trends in $|V|$ can therefore be used to yield S. However, trends in $|V|$ are strongly influenced by trends in data reliability whenever the mean seasonal vector wind ($\overline{V}$) is close to zero. In the early years of the historical record, less reliable data introduce erroneous outliers which raise the mean value of $|V|$. So reliable unbiased estimates of the trend in $|V|$ cannot be made. However, it is possible to make an unbiased estimate of the trend in the seasonal vector wind (V), and use this trend as an approximation for the trend in $|V|$. In order to assess the accuracy of this approximation, consider a vector wind time series to be made up of: trend in $|V|$, $\overline{V}$, and white noise. Figure B1 assumes the white noise to have a standard deviation of 0.75 m s^{-1} (observed order of magnitude for seasonal zonal wind) and the trend of $|V|$ to be 0.005 m s^{-1} yr^{-1} (consistent with that proposed by Cardone et al). The trend in V tends to 0.005 m s^{-1} yr^{-1} as $\overline{V}$ becomes different from zero. For $\overline{V}$ = 1 m s^{-1}, the trend in V is a good approximation of the trend in $|V|$, biased low by only about 15%. Series with $\overline{V}$ in the range -1 m s^{-1} to +1 m s^{-1} were judged unsuitable for estimating the trend in $|V|$. Series with $\overline{V}$ < -1 m s^{-1} were used after being multiplied by -1, so that trends in V and $|V|$ were of the same sign.

Acknowledgements. Jon Maybury helped devise and program the geostrophic wind analysis. Discussions with David Parker are always valued. This work is part of an ongoing PhD study under the supervision of Brian Hoskins (Meteorological Department, Reading University) and Chris Folland (Hadley Centre for Climate Prediction and Research, Meteorological Office).

REFERENCES

Afifi, A.A. and Azen, S.P., 1979: Statistical analysis - a computer oriented approach. Second Edition, Academic Press, New York, xx+442pp.

Bartlett, M. S., 1935: Some aspects of the time correlation problem in regard to tests of significance. J. Roy. Stat. Soc., 98, 536-543.

Bottomley, M., Folland, C.K., Hsiung J., Newell R.E. and Parker D.E., 1990: Global Ocean Surface Temperature Atlas (GOSTA). Joint Meteorological Office/Massachusetts Institute of Technology Project. Project supported by US Dept of Energy, US National Science Foundation and US Office of Naval Research. Publication funded by UK Depts of Energy and Environment. pp20+iv and 313 Plates. HMSO, London.

Cardone, V.J., Greenwood, J.G. and Cane, M.A., 1990: On Trends in Historical Marine Wind Data, J Climate, 3, 113-127.

Colman, A.W., 1988: Development of a Sahel rainfall series using CLIMAT data. Long Range Forecasting and Climate Memorandum No. 30, 7pp (unpublished). Available from the National Meteorological Library, Meteorological Office, Bracknell, Berkshire, UK.

Druyan, L.M., 1989: Advances in the study of sub-Saharan drought. Int. J. Climatol., 9, 77-90.

Druyan, L.M. and Koster, R.D., 1989: Sources of Sahel Precipitation for Simulated Drought and Rainy Seasons. J. Clim., 2, 1438-1446.

Folland, C.K., Karl, T.R. and Vinnikov, K. Y., 1990: Observed Climate Variations and Change. Section 7 (pp 195-238) of Climate Change - The IPCC Scientific Assessment. WMO/UNEP IPCC, Cambridge University Press.

Folland, C.K., Palmer, T.N. & Parker, D.E., 1986: Sahel rainfall and worldwide sea temperatures, 1901-85. Nature, 320, 602-607.

Folland, C.K., Owen, J.A., Ward, M.N. and Colman, A.W., 1991: Prediction of Seasonal Rainfall in the Sahel Region of Africa using empirical and dynamical methods. J. Forecasting, 10, 21-56.

Garratt, J.R. 1977: Review of Drag Coefficients over Oceans and Continents. Mon. Wea. Rev., 105, 915-928.

Hastenrath, S., 1984: Interannual variability and annual cycle: mechanisms of circulation and climate in the tropical Atlantic sector. Mon. Wea. Rev., 112, 1097-1107.

Janicot, S., 1991. Spatio-Temporal Variability of West African Rainfall. J. Climate, in press.

Kendal, M. G. and Stuart, A., 1961: The Advanced Theory of Statistics, Volume 2: Inference and Relationship. Charles Griffin and Co. Ltd., London, ix+676pp.

Kidson, J.W. and Trenberth, K.E., 1988: Effects of missing data on monthly mean general circulation statistics. J. Climate, 1, 1261-1275.

Lamb, P.J., 1978: Large-scale tropical Atlantic surface circulation patterns associated with Subsaharan weather anomalies. Tellus, 30, 240-251.

Lough, J.M., 1986: Tropical Atlantic sea surface temperatures and rainfall variations in Subsaharan Africa. Mon. Wea. Rev., 114, 561-570.

Meehl, G.A., 1987: The Annual Cycle and Interannual Variability in the Tropical Pacific and Indian Ocean Regions. Mon. Wea. Rev., 115, 27-50.

Ng, C. N. and Young, P. C., 1990: Recursive Estimation and Forecasting of Non-stationary Time series. J. Forecasting, 9, 173-204.

Nicholson, S.E., 1985: Sub-Saharan rainfall 1981-84. J. Clim. Appl. Met., 24, 1388-1391.

Nicholson, S.E., 1980: The nature of rainfall fluctuations in sub-tropical West Africa. Mon. Wea. Rev., 108, 473-487.

Palmer, T.N., 1986: Influence of the Atlantic, Pacific and Indian Oceans on Sahel rainfall. Nature, 322, 251-253.

Palmer, T.N., Brankovic, C, Viterbo, P. and Miller, M.J.: Modelling Interannual Variations of Summer Monsoons. J. Climate, in press.

Parker, D.E., 1984: The Statistical effects of incomplete sampling of coherent data series. J. Climatol., 4, 445-449

Ramage, C.S., 1987: Secular changes in reported surface wind speeds over the ocean. J. Clim. Appl. Met., 26, 525-528.

Riehl, H, 1979: Climate and Weather in the Tropics. Academic Press, London, xii+611pp

Ropelewski, C.F. and Halpert, M.S., 1987: Global and Regional Scale precipitation patterns associated with the El Nino / Southern Oscillation. Mon. Wea. Rev., 115, 1606-1626.

Ropelewski, C.F. and Halpert, M.S., 1989: Precipitation patterns associated with the high index phase of the Southern Oscillation. J. Climate, 2, 268-284.

Rowell, D.P, Folland, C.K., Maskell, K.M., Owen, J.A. and Ward, M.N., 1991: Causes and Predictability of Sahel Rainfall Variability, Climate Research Technical Note No. 12, Available from the National Meteorological Library, Meteorological Office, Bracknell, Berkshire, UK. Submitted to Nature.

Ward, M.N., Folland, C.K., Maskell, K., Rowell, D.P. and Colman, A.W. 1990: Understanding and predicting seasonal rainfall in sub-Saharan Africa. Proceedings of the Third WMO Symposium on Meteorological Aspects of Tropical Droughts with the emphasis on Long-Range Forecasting, 30 April - 4 May, 1990, Niamey, Niger; TMRPR 36, WMO/TD 353, pp 157-162.

Wolter, K., 1989: Modes of tropical circulation, Southern Oscillation, and Sahel rainfall anomalies. J. Climate, 2, 149-172.

Woodruff, S.D., Slutz, R.J., Jenne, R.L. and Steurer, P.M., 1987: A comprehensive ocean-atmosphere data set. Bull. Am. Met. Soc., 68, 1239-1250.

Wright, P.B., 1988: On the reality of climatic changes in wind over the Pacific. J. Climatol., 8, 521-527.

Young, P.C., Ng, N.C., Lane, K. and Parker, D.E., 1991: Recursive Forecasting, Smoothing and Seasonal Adjustment of Non-Stationary Environmental Data. J. Forecasting, 10, 57-90.

Figures

FIG. 1. (a) Distribution of stations used by Nicholson (1985), and the boundary of the Sahel using Nicholson's definition (mean annual rainfall 100mm-400mm). (b) Standardised annual rainfall anomalies for the Sahel, 1901-1990. Values to 1984 are from Nicholson (1985); 1985-1990 values are based on CLIMAT reports. Trend component (solid line) fitted using Integrated Random Walk smoothing algorithm described in Ng and Young (1990) and Young et al (1991) with 50% cut-off frequency set to about 10 years. (c) The number of stations available in each year.

FIG. 2. The difference between the rise in the observed wind and the rise in the derived geostrophic wind over 1949-1988, expressed as a percentage of the mean observed wind (S in Eq. (5)). Values shown are a weighted average of many estimates of S calculated on the 2° lat x 2° lon scale (see text for more details).

FIG. 3. 1949-1988 July-September anomalies of uncorrected zonal wind (dashed line) and corrected zonal wind (solid line) for 10° x 10° box centred at 45°W, 15°N. Crosses are the sea level pressure (SLP) anomaly difference for 10° x 10° boxes: (45°W, 5°N) MINUS (45°W, 15°N). Correlations with SLP difference time series: (i) reported wind, r=0.58 (ii) corrected wind, r=0.66. Linear trend lines: (a) = Uncorrected Wind, (b) = SLP difference, (c) = Corrected wind.

FIG. 4. Composite analyses for July-September means, Sahel wet (1950, 1952, 1953, 1954, 1958) minus Sahel dry (1972, 1973, 1982, 1983, 1984) for: (a) Sea Surface Temperature, (b) Sea Level Pressure, (c) Corrected vector wind, (d) Uncorrected vector wind. Shaded values in (a) and (b) are significant at the 10% level according to a t-test.

FIG. 5 July-September means, 1988 (Sahel average) minus 1987 (Sahel Dry) for: (a) Sea Surface Temperature, (b) Sea Level Pressure, (c) Corrected vector wind (because there is little difference in time between 1988 and 1987, the corrected and uncorrected wind maps are almost identical, hence the uncorrected is not shown).

FIG. 6. Correlations (in hundredths) between 10° x 10° sea level pressure anomalies for July-September and standardized Sahel rainfall series 1949-1988. Correlations significant at the 5% level are shaded.

FIG. 7. Covariance Eigenvectors (EOFs) of seasonal 10° x 10° sea surface temperature anomalies for 1901-1980. (a) Unrotated EOF 2, (b) Unrotated EOF 3, (c) Rotated EOF 2 (derived by VARIMAX rotation of EOFs 4-13). (Taken from Folland et al, 1991).

FIG. A1. Identification of those pairs of boxes that qualify as candidates for providing an estimate of mean SLP gradient across box i for a given season. Each pair of nearby 2° x 2° boxes are considered. The point c is the centre of box i, a and b are the respective mean locations of the season's SLP observations in the pair of boxes being considered, m is the mid-point of the line joining a and b, θ is the angle between the "preferred axis" and the line joining a and b.

FIG. A2. Preferred Axis along which a pressure gradient was sought. Arrow indicates the axis used for all 2° x 2° boxes contained within the box marked by a solid line. Where a preferred axis is not specified, it was taken to be 15° clockwise from the north-south direction in the Northern Hemisphere, 15° anticlockwise in the Southern Hemisphere. In any given season, the two boxes used for the pressure gradient estimate were permitted to form an axis up to 20° from the "preferred axis".

FIG. B1. The relationship between the trend in a vector quantity and the trend in its modulus: the graph shown is for a seasonal vector wind (V) with standard deviation 0.75 m s^{-1} and trend in the modulus of V of 0.005 m s^{-1} yr^{-1} (dashed line). The solid line (estimated from Monte Carlo experiments) shows the trend in V as a function of the mean vector wind ($\overline{V}$).

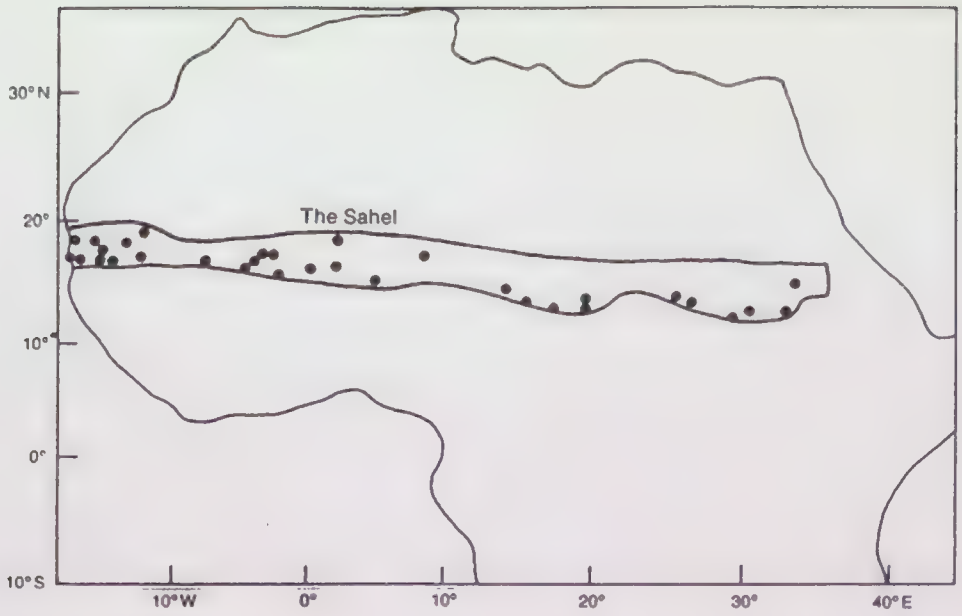

(a)

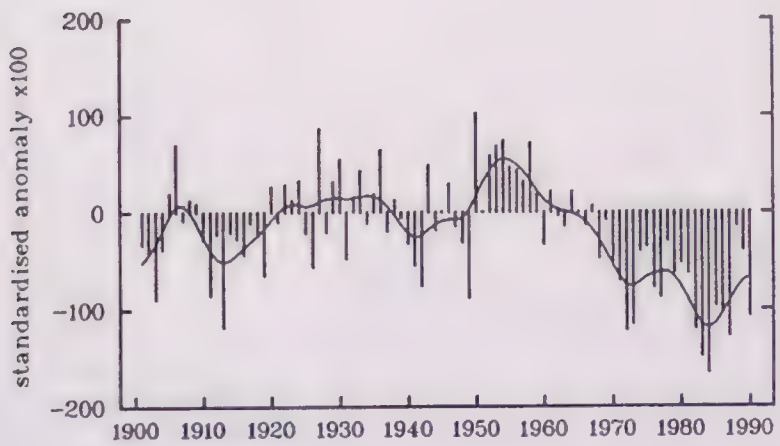

(b)

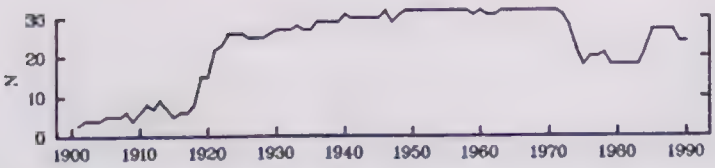

(c)

FIG. 1. (a) Distribution of stations used by Nicholson (1985), and the boundary of the Sahel using Nicholson's definition (mean annual rainfall 100mm-400mm). (b) Standardised annual rainfall anomalies for the Sahel, 1901-1990. Values to 1984 are from Nicholson (1985); 1985-1990 values are based on CLIMAT reports. Trend component (solid line) fitted using Integrated Random Walk smoothing algorithm described in Ng and Young (1990) and Young et al (1991) with 50% cut-off frequency set to about 10 years. (c) The number of stations available in each year.

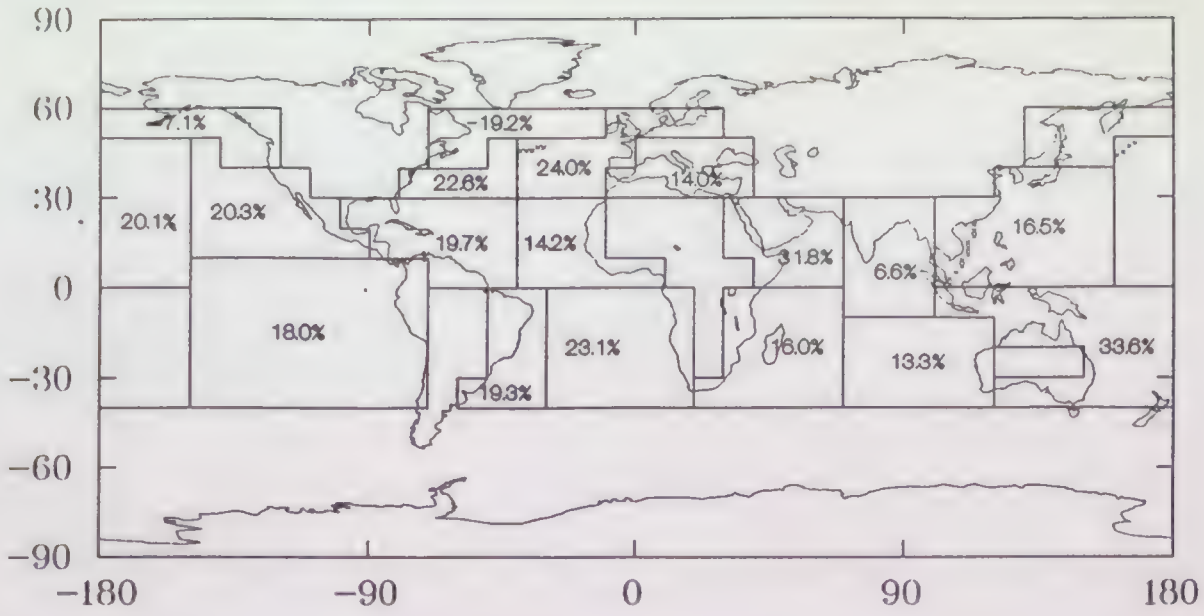

FIG. 2. The difference between the rise in the observed wind and the rise in the derived geostrophic wind over 1949-1988, expressed as a percentage of the mean observed wind (S in Eq. (5)). Values shown are a weighted average of many estimates of S calculated on the 2° lat x 2° lon scale (see text for more details).

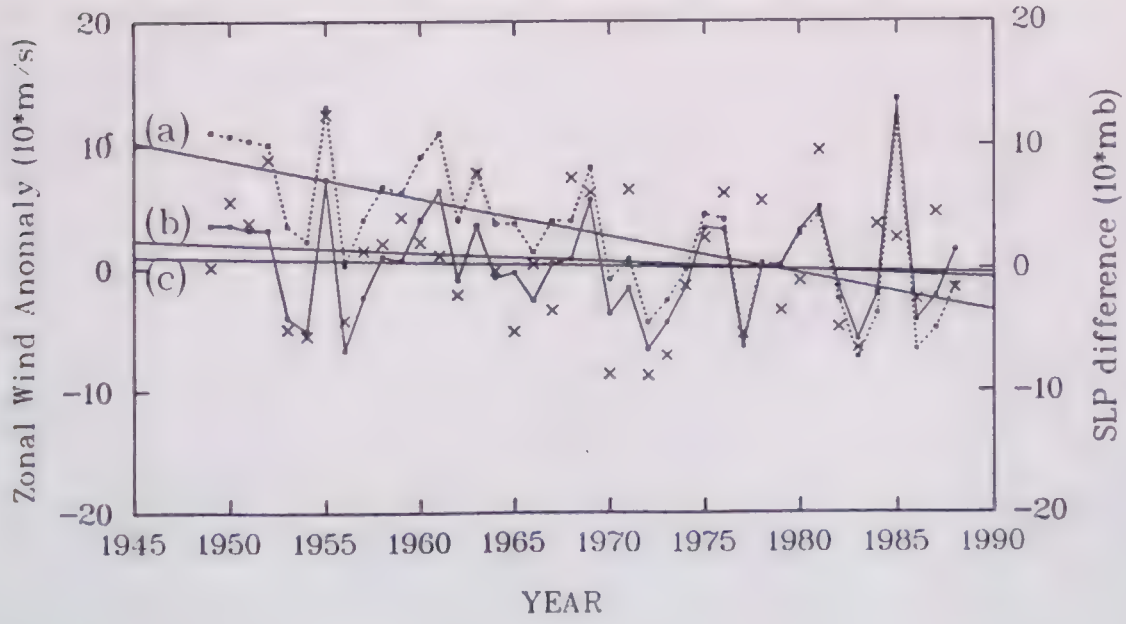

FIG. 3. 1949-1988 July-September anomalies of uncorrected zonal wind (dashed line) and corrected zonal wind (solid line) for 10° x 10° box centred at 45°W, 15°N. Crosses are the sea level pressure (SLP) anomaly difference for 10° x 10° boxes: (45°W, 5°N) MINUS (45°W, 15°N). Correlations with SLP difference time series: (i) reported wind, r=0.58 (ii) corrected wind, r=0.66. Linear trend lines: (a) = Uncorrected Wind, (b) = SLP difference, (c) = Corrected wind.

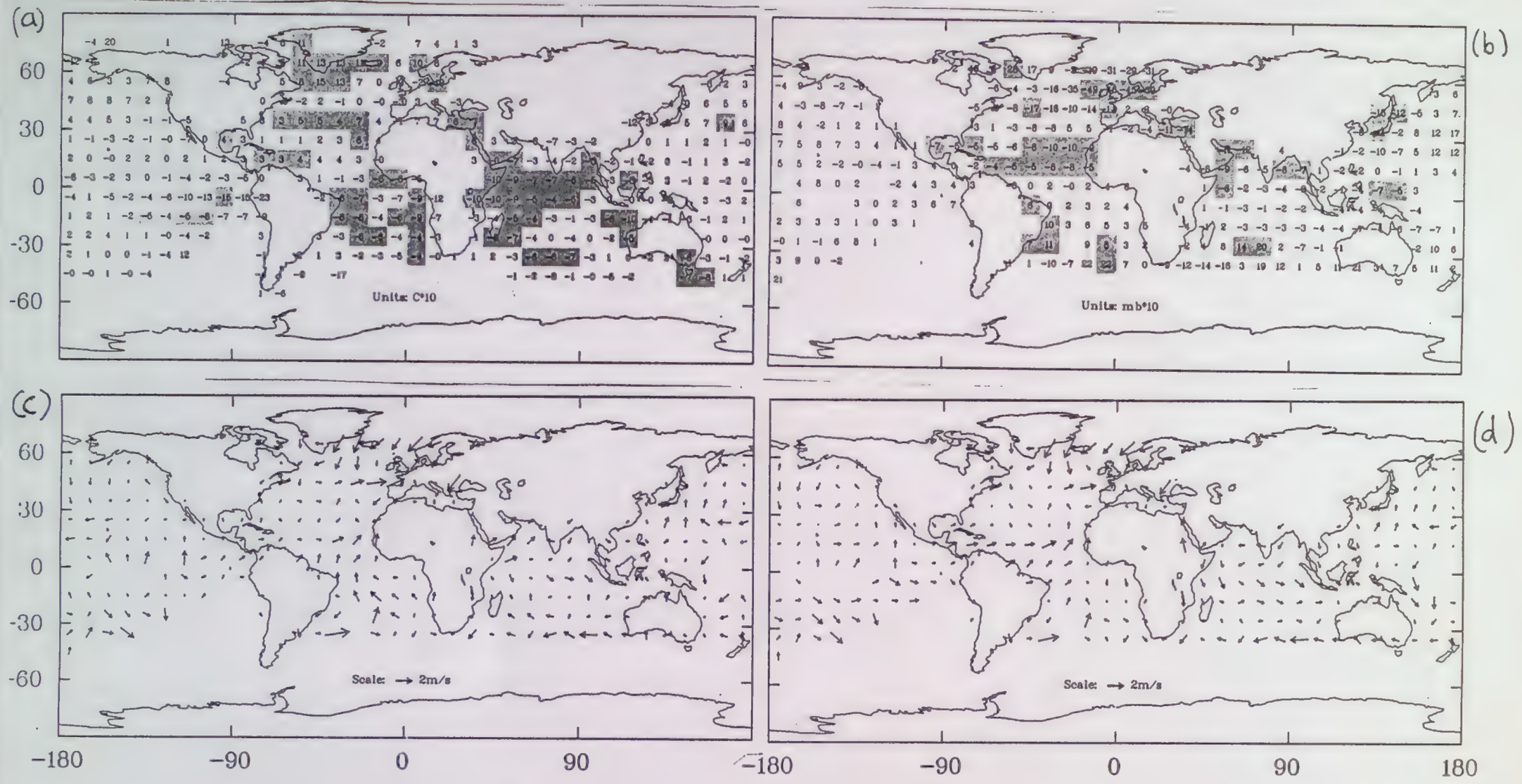

FIG. 4. Composite analyses for July-September means, Sahel wet (1950, 1952, 1953, 1954, 1958) minus Sahel dry (1972, 1973, 1982, 1983, 1984) for: (a) Sea Surface Temperature, (b) Sea Level Pressure, (c) Corrected vector wind, (d) Uncorrected vector wind. Shaded values in (a) and (b) are significant at the 10% level according to a t-test.

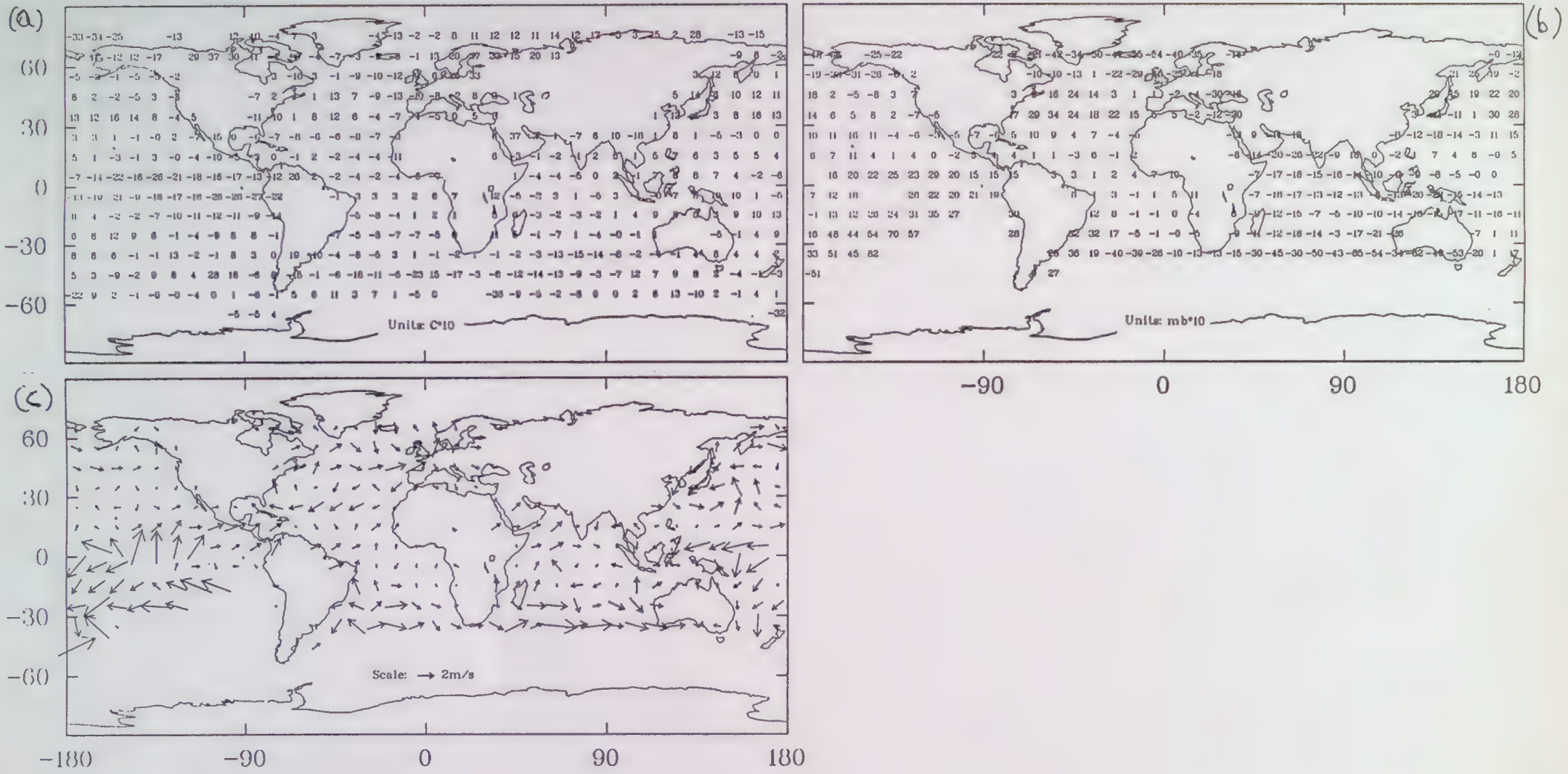

FIG. 5 July-September means, 1988 (Sahel average) minus 1987 (Sahel Dry) for: (a) Sea Surface Temperature, (b) Sea Level Pressure, (c) Corrected vector wind (because there is little difference in time between 1988 and 1987, the corrected and uncorrected wind maps are almost identical, hence the uncorrected is not shown).

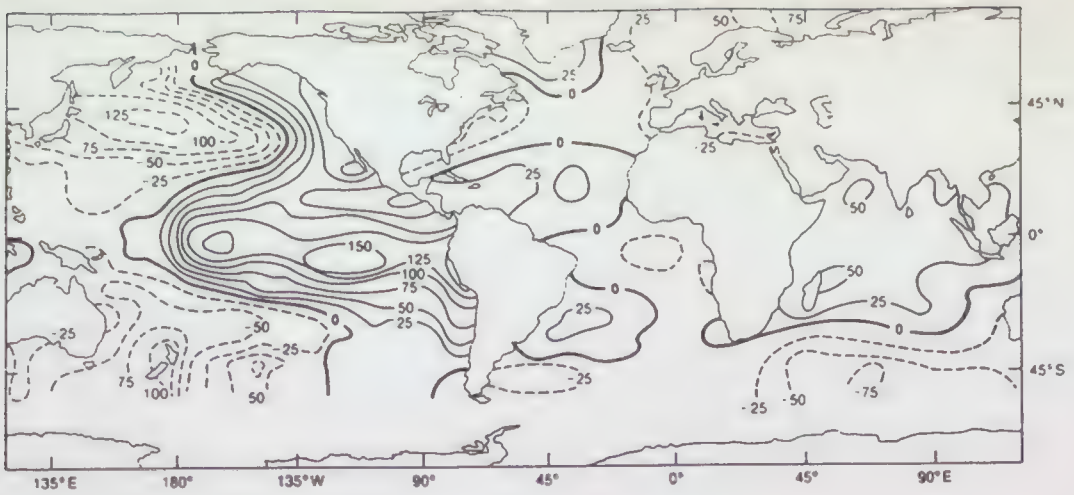

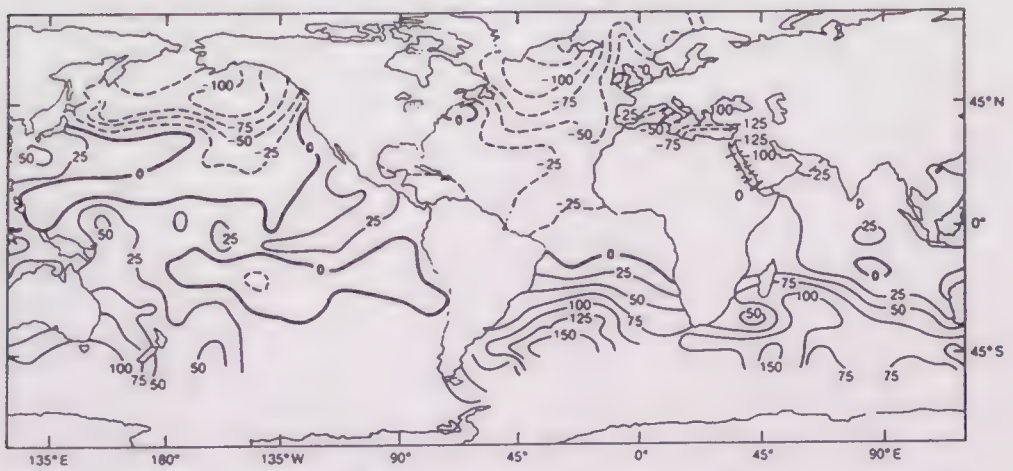

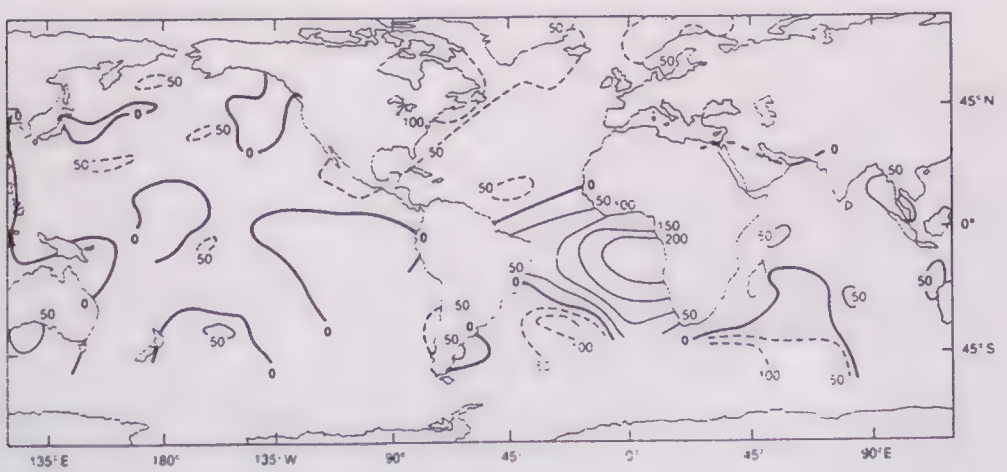

FIG. 7. Covariance Eigenvectors (EOFs) of seasonal 10^{o} x 10^{o} sea surface temperature anomalies for 1901-1980. (a) Unrotated EOF 2, (b) Unrotated EOF 3, (c) Rotated EOF 2 (derived by VARIMAX rotation of EOFs 4-13). (Taken from Folland et al, 1991).

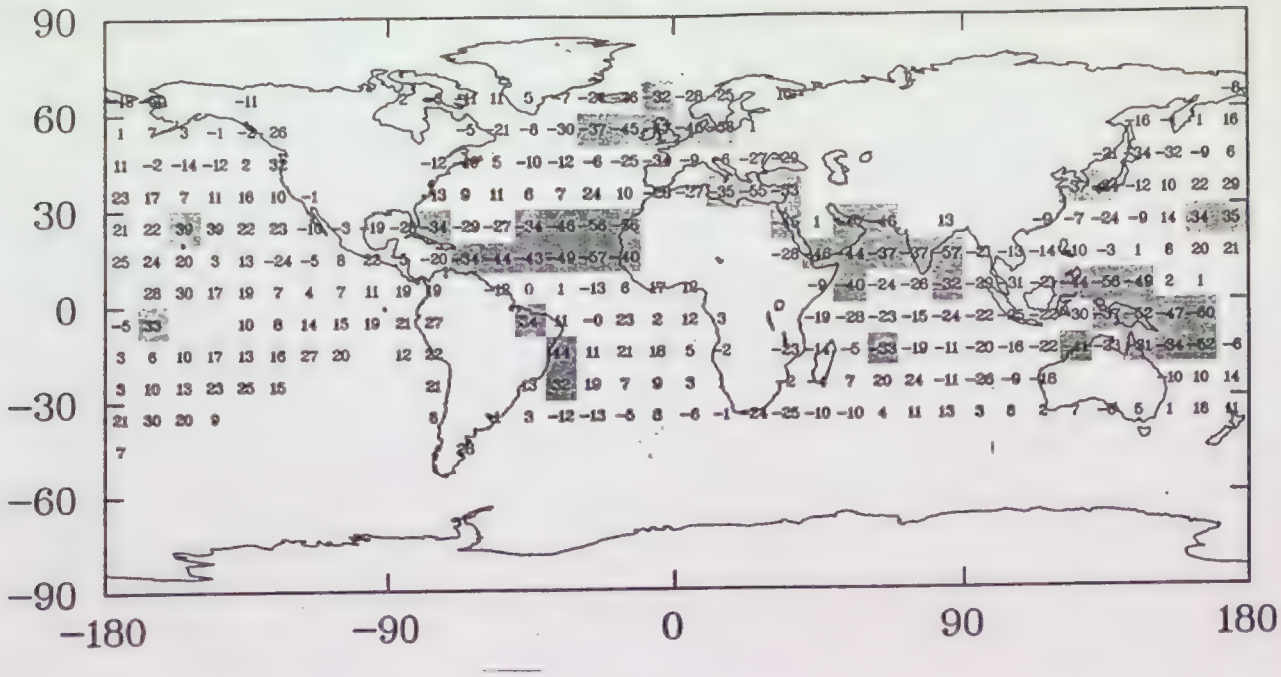

FIG. 6. Correlations (in hundredths) between 10° x 10° sea level pressure anomalies for July-September and standardized Sahel rainfall series 1949-1988. Correlations significant at the 5% level are shaded.

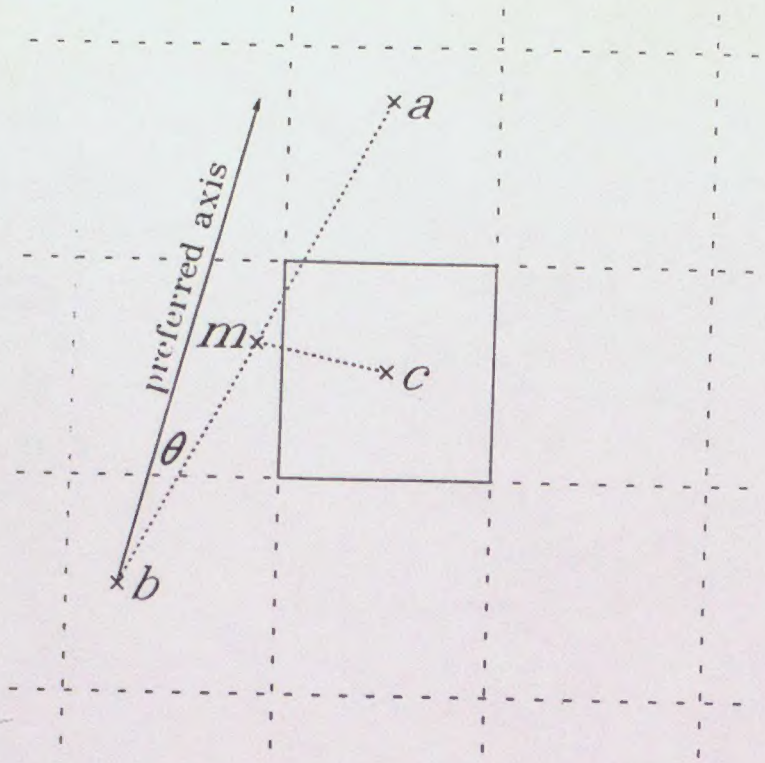

FIG. A1. Identification of those pairs of boxes that qualify as candidates for providing an estimate of mean SLP gradient across box i for a given season. Each pair of nearby 2^{o} x 2^{o} boxes are considered. The point c is the centre of box i, a and b are the respective mean locations of the season's SLP observations in the pair of boxes being considered, m is the mid-point of the line joining a and b, θ is the angle between the "preferred axis" and the line joining a and b.

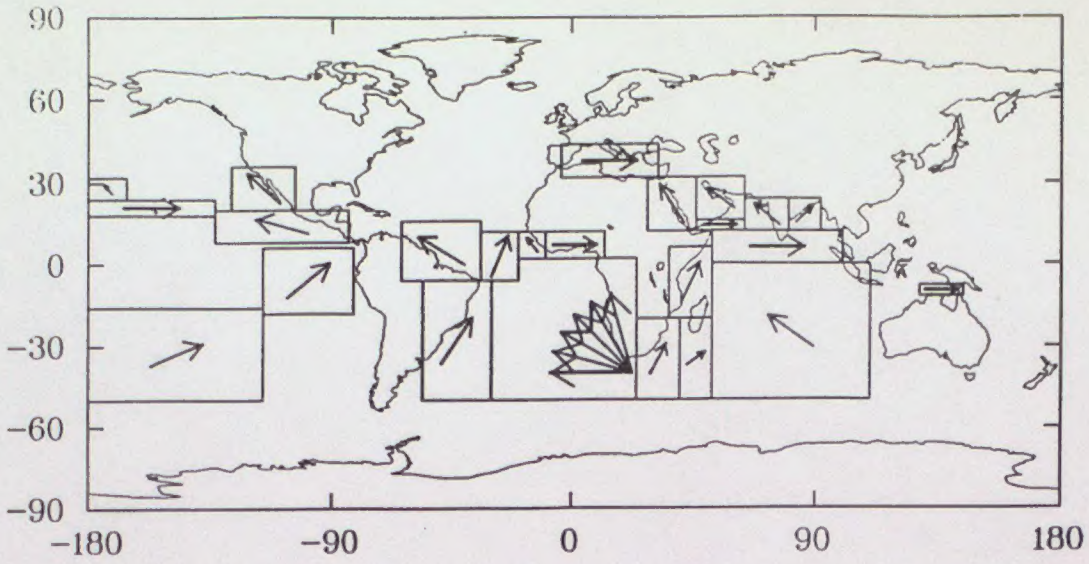

FIG. A2. Preferred Axis along which a pressure gradient was sought. Arrow indicates the axis used for all 2° x 2° boxes contained within the box marked by a solid line. Where a preferred axis is not specified, it was taken to be 15° clockwise from the north-south direction in the Northern Hemisphere, 15° anticlockwise in the Southern Hemisphere. In any given season, the two boxes used for the pressure gradient estimate were permitted to form an axis up to 20° from the "preferred axis".

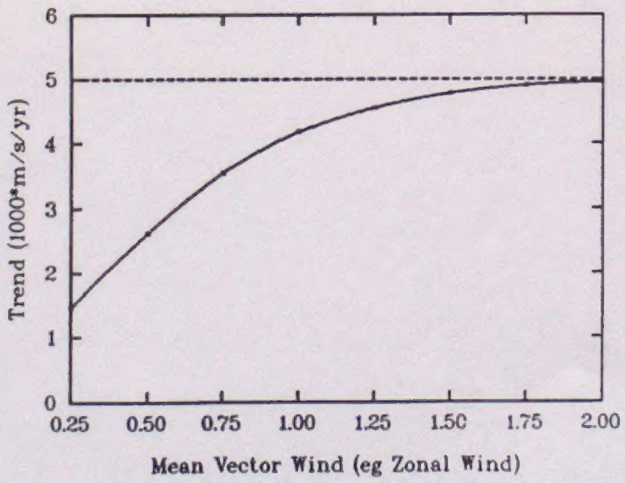

FIG. B1. The relationship between the trend in a vector quantity and the trend in its modulus: the graph shown is for a seasonal vector wind (V) with standard deviation 0.75 m s^{-1} and trend in the modulus of V of 0.005 m s^{-1} yr^{-1} (dashed line). The solid line (estimated from Monte Carlo experiments) shows the trend in V as a function of the mean vector wind ($\overline{V}$).

CLIMATE RESEARCH TECHNICAL NOTES

CRTN 1	Oct 1990	Estimates of the sensitivity of climate to vegetation changes using the Penman-Monteith equation. P R Rowntree
CRTN 2	Oct 1990	An ocean general circulation model of the Indian Ocean for hindcasting studies. D J Carrington
CRTN 3	Oct 1990	Simulation of the tropical diurnal cycle in a climate model. D P Rowell
CRTN 4	Oct 1990	Low frequency variability of the oceans. C K Folland, A Colman, D E Parker and A Bevan
CRTN 5	Dec 1990	A comparison of 11-level General Circulation Model Simulations with observations in the East Sahel. K Maskell
CRTN 6	Dec 1990	Climate Change Prediction. J F B Mitchell and Qing-cun Zeng
CRTN 7	Jan 1991	Deforestation of Amazonia - modelling the effects of albedo change. M F Mylne and P R Rowntree
CRTN 8	Jan 1991	The role of observations in climate prediction and research. D J Carson
CRTN 9	Mar 1991	The greenhouse effect and its likely consequences for climate change. D J Carson
CRTN 10	Apr 1991	Use of wind stresses from operational N.W.P. models to force an O.G.C.M. of the Indian Ocean. D J Carrington
CRTN 11	Jun 1991	A new daily Central England Temperature series, 1772-1991. D E Parker, T P Legg and C K Folland
CRTN 12	Jul 1991	Causes and predictability of Sahel rainfall variability. D P Rowell, C K Folland, K Maskell, J A Owen, M N Ward
CRTN 13	Jul 1991	Modelling changes in climate due to enhanced CO_2, the role of atmospheric dynamics, cloud and moisture. C A Senior, J F B Mitchell, H Le Treut and Z-X Li

CLIMATE RESEARCH TECHNICAL NOTES

CRTN 14	Sep 1991	Sea temperature bucket models used to correct historical SST data in the Meteorological Office. C K Folland
CRTN 15	Aug 1991	Modelling climate change, and some potential effects on agriculture in the U.K. P R Rowntree, B A Callander and J Cochrane
CRTN 16	Aug 1991	The Boreal Forests and Climate G Thomas and P R Rowntree
CRTN 17	Aug 1991	Development of a Stratosphere-Troposphere Data Assimilation System. R Swinbank.
CRTN 18	Sep 1991	A study of asynchronous coupling using a simple climate model. M K Davey.
CRTN 19	Sep 1991	The Oceanic Carbon Cycle. N K Taylor
CRTN 20	Nov 1991	Worldwide ocean-atmosphere surface fields in Sahel wet and dry years using provisionally corrected surface wind data. M N Ward